

Dependence of the glass transition and jamming densities on spatial dimension

Monoj Adhikari,¹ Smarajit Karmakar,² and Srikanth Sastry^{1,*}

¹Theoretical Science Unit, Jawaharlal Nehru Centre for Advanced Scientific Research, Jakkur Campus, 560064 Bengaluru, India

²TIFR Center for Interdisciplinary Science, Tata Institute of Fundamental Research, RR District, Hyderabad, 500046, Telangana, India,

We investigate the dynamics of soft sphere liquids through computer simulations for spatial dimensions from $d = 3$ to 8, over a wide range of temperatures and densities. Employing a scaling of density-temperature dependent relaxation times, we precisely identify the density ϕ_0 which marks the ideal glass transition in the hard sphere limit, and a crossover from sub- to super-Arrhenius temperature dependence. The difference between ϕ_0 and the athermal jamming density ϕ_J , small in 3 and 4 dimensions, increases with dimension, with $\phi_0 > \phi_J$ for $d > 4$. We compare our results with recent theoretical calculations.

Introduction: Fluid states of matter can transform to rigid, amorphous solids through the glass transition or the jamming transition. The glass transition describes the transition to disordered solid states typically in molecular systems upon a decrease in temperature, whose nature has been intensely investigated over several decades [1–5]. The jamming transition has likewise been widely investigated in *athermal* systems, typified by granular matter [6–8]. Their relationship has also been the subject of considerable research [9]. Whereas molecular glass formers and granular matter represent cases which exhibit one or the other of these phenomena, several systems, such as colloidal suspensions, in principle exhibit both phenomena, and their interplay is important, *e.g.* in their rheology [10]. An idealised system in which both phenomena have been investigated in detail is the hard sphere system. Theoretical investigations over the last decade, extending the framework of the random first order transition (RFOT) theory [11–13], have focused on the hard sphere system, and a unified mean field description of both these phenomena have been developed in the limit of infinite dimensions [9, 14, 15]. These developments have naturally led to investigations of how the infinite dimensional results relate to behaviour in finite dimensions. An appealing and systematic approach to addressing questions in this regard is to study the effect of spatial dimensionality on the glass transition and jamming phenomenology, which have been pursued for hard particle systems extensively [9, 15–21]. In particular, the relationship between the glass transition and jamming transition has been investigated [15, 16]. In addition to systems of hard spheres, a small number of other studies have investigated the role of dimensionality in determining aspects of glassy dynamics [22–26], such as dynamical heterogeneity in a binary mixture of the Lennard-Jones particles as a function of temperature. A more extensive investigation of the dependence on spatial dimensionality in systems where both thermal and density effects play a role are thus of great interest. In the present work, we study soft sphere assemblies interacting with a harmonic

potential by investigating the dynamics at different densities and temperatures.

In the zero-temperature limit, the behavior of this system approaches the density-controlled hard sphere model, while it is similar to thermally driven fluids at high density and finite temperature. In the hard sphere limit, the system *jams*, losing the ability to flow, at a critical density, ϕ_J , *via* the non-equilibrium jamming transition [27, 28]. Several works [28–35] have considered and demonstrated the scenario that the jamming density is not unique, but can occur over a range of densities. In turn, the range of jamming densities is associated with a line of glass transition densities (kinetically determined or otherwise, as in mean field results [9, 14]) ending with a *Kauzmann* density ϕ_0 , which may be expected to be the relevant density for the divergence of relaxation times. The relationship between the jamming and Kauzmann densities have been investigated, with varying conclusions regarding the relative values of ϕ_J and ϕ_0 [16, 36–39]. Several studies [9, 15, 32, 38, 40, 41] also indicate that the relationship between these two transition densities depends on dimensionality.

In [36, 37], the relaxation times were studied for the same model we consider, in three dimensions. With increasing density, relaxation times exhibit a cross over from sub-Arrhenius to super-Arrhenius temperature dependence. Relaxation times were analysed through a scaling function that assumes a divergence for the hard sphere systems at a density ϕ_0 , and by defining an effective hard sphere diameter at finite temperatures [42], to obtain two distinct scaling collapses across ϕ_0 . The estimate of ϕ_0 thus obtained is found to be very close to ϕ_J , the jamming point, although the meaning of the two densities was clearly distinguished.

In the present work, we perform extensive molecular dynamics simulations for a wide range of ϕ, T values in different spatial dimensions ranging from $d = 3$ to 8. We perform a scaling analysis similar to [36, 37] but with a newly proposed scaling function, to obtain ϕ_0 as a function of d . We obtain jamming densities following

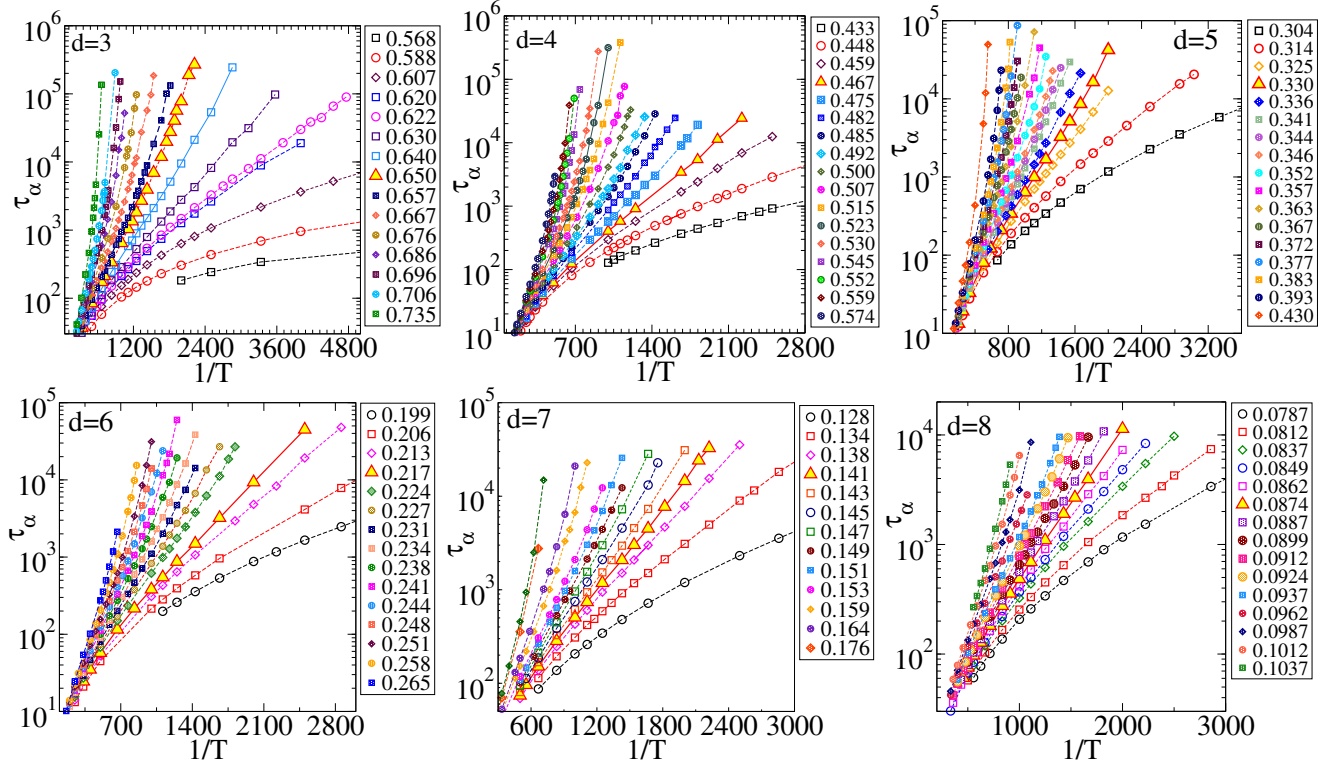


FIG. 1. Relaxation times as a function of inverse temperature are plotted in a semi-log scale for several densities in different dimensions. Data shown with filled symbols correspond to densities at which super-Arrhenius dependence is observed.

the analysis in [27, 28]. Our results clearly demonstrate that $\phi_0 > \phi_J$ for $d > 4$, with ϕ_0/ϕ_J increasing with d , as may be expected from mean field results [9, 14, 15].

Simulations details: We study a 50 : 50 binary mixture of spheres of size ratio 1.4, interacting with a harmonic potential as a model glass former [43]:

$$V_{\alpha\beta}(r) = \frac{\epsilon_{\alpha\beta}}{2} \left(1 - \frac{r}{\sigma_{\alpha\beta}}\right)^2, \quad r_{\alpha\beta} \leq \sigma_{\alpha\beta} \quad (1)$$

and $V_{\alpha\beta}(r) = 0$ for $r_{\alpha\beta} > \sigma_{\alpha\beta}$, where $\alpha, \beta \in (A, B)$, indicates the type of particle. The system size varies from 1000 to 5000 depending on the spatial dimensions, with the linear extent of the simulated volume, $L > 2\sigma_{BB}$ in all dimensions. We investigate the dynamics at 10 – 14 densities (with 1 - 2 independent samples each) around the jamming density. The volume fraction, or density, $\phi = \rho V_d$ where $V_d = 2^{-d} \frac{\pi^{d/2}}{\Gamma(1+d/2)} ((c_A \sigma_{AA}^d + c_B \sigma_{BB}^d))$, $c_A = c_B = 1/2$, is the average volume per sphere in d dimensions, $\rho = \frac{N}{V}$ is the number density, N is the number of particles, and V is the volume. Molecular dynamics (MD) simulations are performed in a cubic box with the periodic boundary conditions, employing the constant temperature integration in [44], with time step $dt = 0.01$. Each independent run is of length $> 100\tau_\alpha$ where relaxation time τ_α is computed from the overlap

function $q(t)$ (for B particles) as $\langle q(t = \tau_\alpha) \rangle = 1/e$, with

$$q(t) = \frac{1}{N_B} \sum_{i=1}^{N_B} w(|\mathbf{r}_j(t_0) - \mathbf{r}_i(t + t_0)|), \quad (2)$$

where $w(x) = 1$ if $x < a$ and 0 otherwise. In Fig. 1, the relaxation time is plotted as a function of temperature for various densities for 3 – 8 dimensions. Additional details are provided in the Supplemental Material (SM) [45]

Results: Considering an expression for relaxation times for hard sphere fluids of the form $\sqrt{T}\tau_\alpha^{hs} \sim \exp\left[\frac{A}{(\phi_0 - \phi)^\delta}\right]$, Berthier and Witten [36] analysed relaxation times for soft spheres by defining a temperature dependent effective volume fraction of the form $\phi_{eff} = \phi - aT^{\mu/2}$, which leads to the scaling form

$$\sqrt{T}\tau_\alpha(\phi, T) \sim \exp\left[\left(\frac{A}{|\phi_0 - \phi|^\delta}\right) F_\pm\left(\frac{|\phi_0 - \phi|^{\frac{2}{\mu}}}{T}\right)\right], \quad (3)$$

where $F_\pm(x)$ refers to the scaling function for the super-Arrhenius and the sub-Arrhenius branch of the scaling function and μ, δ and ϕ_0 are adjustable parameters. Plotting $|\phi_0 - \phi|^\delta \log(\tau_\alpha)$ against $|\phi_0 - \phi|^{\frac{2}{\mu}}/T$, with suitable choices of the parameters, a data collapse on to two branches above and below ϕ_0 is obtained. The values of $\phi_0 = 0.635$ and $\delta = 2.2$ were determined from such a procedure, with the δ value being in close agreement with

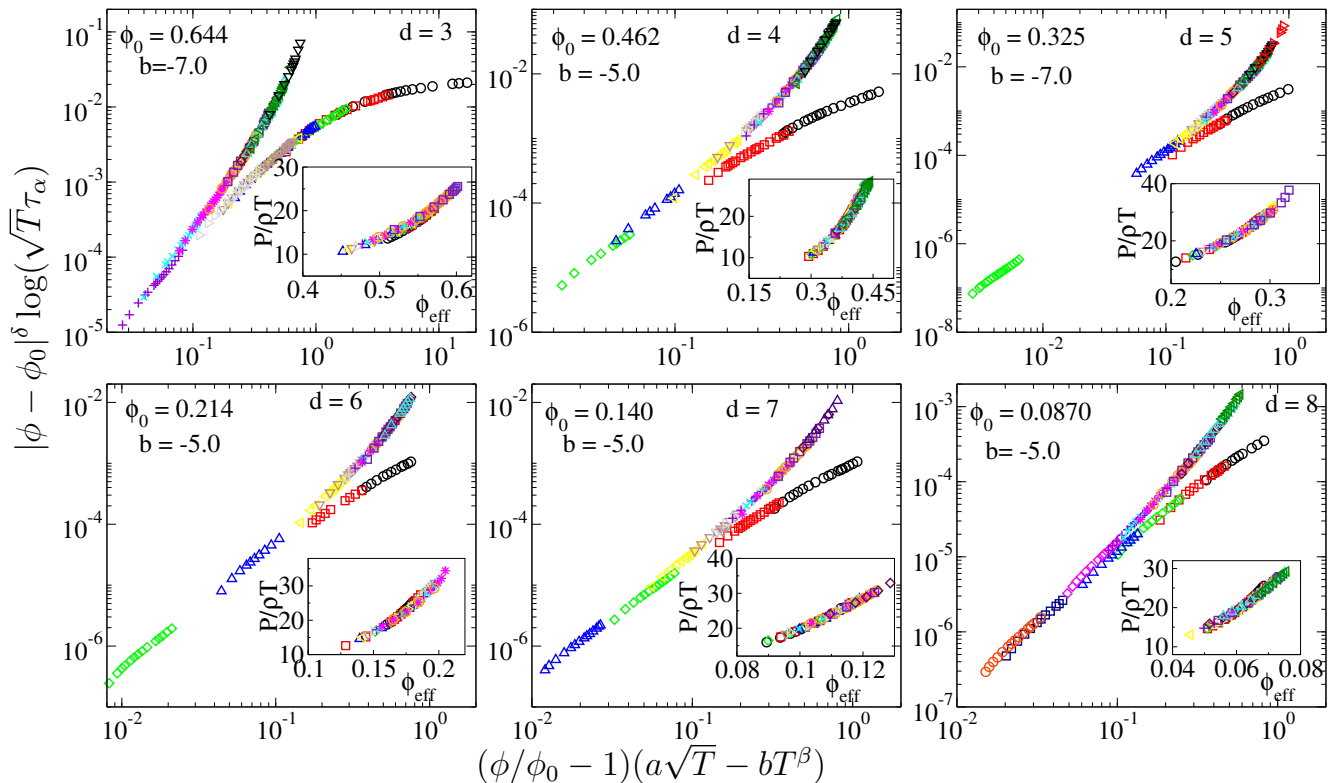


FIG. 2. Scaling plot of relaxation times for 3 – 8 spatial dimension. As explained in the text, coefficients a, b and exponent β describe the effective volume fraction ϕ_{eff} . Of these, we use fixed values of $a = d\sqrt{\pi}/2$ (see SM) and vary $b, \beta > 0.5$ to obtain collapse of pressures on to a single curve, $P/\rho T = f(\phi_{eff})$ (shown in the insets). Best data collapse is obtained around $\beta = 0.7$ (which we keep fixed), and the b values are indicated in the legends. Keeping $\delta = 2$ fixed, we vary ϕ_0 as the single fit parameter to obtain scaling plots of relaxation times τ_α shown.

experimental and simulation results for colloidal hard spheres and theoretical results [46–48]. The estimated ϕ_0 is close to but distinct from the jamming density of $\phi_J = 0.648$ estimated for the binary mixture studied in [27, 28, 36] and here.

Recently, the same scaling analysis has been revisited in [49], with the conclusion that if one considers ϕ_0, δ and μ as free parameters, a good scaling collapse of comparable quality to [36] could be obtained for significantly different sets of parameter values. Further, the scaling form in Eq. 3 requires $\mu\delta/2 = 1$ in order to obtain the expected Arrhenius form at density ϕ_0 , but imposing such a constraint does not lead to the best data collapse [36], as we independently verify. It is thus desirable to explore alternate scaling functions, which we do in this work based on the evaluation of an effective diameter following the prescription in [50]. We compare our results to analysis employing Eq. 3, and obtain consistent estimates of ϕ_0 .

Following [50], the expression for the effective diameter with only temperature dependent corrections can be written as $\sigma_{eff} = \int_0^\sigma [1 - \exp(-\beta u(r))] dr$, leading to $\sigma_{eff} \approx \sigma \left[1 - \frac{1}{2} \sqrt{\pi/\beta}\right]$. In turn, the effective volume

fraction in dimension d can be approximated as

$$\phi_{eff} \approx \phi \left(1 - a \sqrt{T} + b T^\beta\right) \quad (4)$$

where $a = d\sqrt{\pi}/2$, and the term bT^β approximates terms of $\mathcal{O}(T)$ and higher. Employing the effective ϕ in the expression for the hard sphere relaxation times, we write

$$\sqrt{T}\tau_\alpha(\phi, T) \sim \exp \left[\frac{A}{|\phi_0 - \phi|^\delta} F_\pm \left(\frac{|\frac{\phi_0}{\phi} - 1|}{a\sqrt{T} - bT^\beta} \right) \right]. \quad (5)$$

An Arrhenius form of the relaxation times at finite T and $\phi = \phi_0$ requires δ to be 2, which we employ. Rather than estimate b, β and ϕ_0 through a scaling analysis of τ_α , we first require that $P/\rho T$ where P is the pressure is a unique function of ϕ_{eff} and estimate b and β from the data collapse of $P/\rho T$ (shown in the insets of Fig. 2). Scaling collapse of τ_α through Eq. 5, shown in Fig. 2, is used to estimate the remaining parameter ϕ_0 . Additional details regarding the data collapse procedure including error analysis and justification of the choice $\delta = 2$, are provided in the SM.

We next estimate the jamming densities following the protocol employed in [28], wherein initially random configurations are compressed till the energy reaches 10^{-5} ,

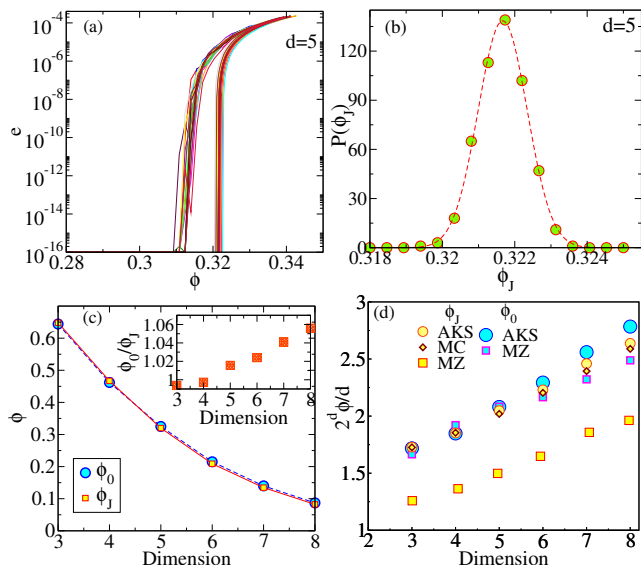


FIG. 3. (a): The energies during compression-decompression cycles of energy-minimized configurations plotted as a function of volume fraction for $d = 5$. Data are shown for 50 independent samples. (b) The histogram of jamming densities for $d = 5$. (c) The jamming density, ϕ_J and the glass transition density, ϕ_0 , plotted as a function of spatial dimension. Inset: Ratio of ϕ_0 and ϕ_J , plotted as a function of spatial dimension. (d) Comparison of ϕ_0 and ϕ_J values from the present work (AKS) with previous simulation [51] (MC) and theoretical calculations [15] (MZ) using the Percus-Yevick closure.

and decompressed till the energy decreases below 10^{-16} , at the jamming density (see SM for additional details). Fig. 3(a) illustrates the protocol for $d = 5$ (corresponding data for all dimensions are shown in the SM). Based on the initial configuration used, the ϕ_J we estimate corresponds to the low density limit of the range over which jamming can take place [27, 28]. The procedure is applied to 1000 independent initial configurations, and the histogram of jamming densities obtained is shown in Fig. 3(b). The average jamming density ϕ_J is shown in Fig. 3(c) (also tabulated in Table I), along with estimates of ϕ_0 obtained above. The ratio ϕ_0/ϕ_J , shown in the inset, increases with d , with $\phi_0 > \phi_J$ for $d > 4$, whereas for $d = 3, 4$, $\phi_0 < \phi_J$, with the two values being very close. The jamming densities ϕ_J we obtain are very similar to, but slightly larger than, those obtained for monodisperse spheres in [20, 51]. In Fig. 3(d), we compare the scaled jamming densities we obtain with those in [51]. We also show the recent theoretical calculations in [15] for the corresponding quantity ϕ_{th} , which shows the same trend as our ϕ_J data, but are smaller (reasons why this may be expected are discussed in [52]). We further show the ϕ_0 values we obtain, along with the corresponding calculated values (Kauzmann density ϕ_K) in [15]. As discussed in [14, 15], $2^d \phi_0/d$ is expected to increase as $\log d$, whereas $2^d \phi_J/d \rightarrow 6.2581$ as $d \rightarrow \infty$. We are not able to quanti-

tatively comment on either prediction, but we note that the values of ϕ_0 calculated in [15] are in near quantitative agreement with our results, whereas the ϕ_J values in [15] underestimate our results as well as those in [20, 51].

d	ϕ_J	ϕ_0
3	0.648 ± 0.0014	0.644 ± 0.003
4	0.467 ± 0.0015	0.462 ± 0.004
5	0.320 ± 0.0008	0.325 ± 0.003
6	0.209 ± 0.0006	0.214 ± 0.002
7	0.1345 ± 0.0004	0.140 ± 0.002
8	0.0824 ± 0.0003	0.0870 ± 0.001

TABLE I. Jamming and glass transition densities ϕ_J and ϕ_0 for dimensions d from 3 to 8. Error bars for ϕ_0 are obtained by considering an increase in the error χ^2 (defined in SM) by 20% of the lowest value. The error bars of ϕ_J is computed from half width at half maximum of the distribution of ϕ_J (shown Fig. 3(b) and the SM).

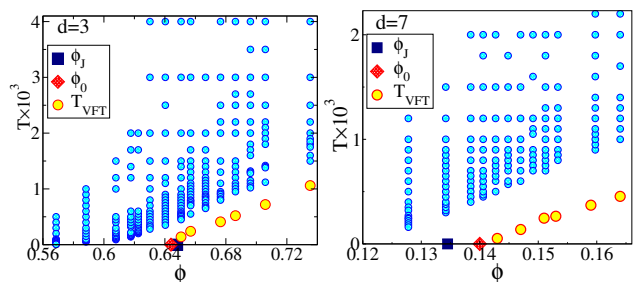


FIG. 4. The jamming and glass transition densities ϕ_J (black square) and ϕ_0 (red diamond) are shown for $d = 3$ and $d = 5$ along with the density dependent glass transition temperatures T_{VFT} (orange circles), and the set of densities and temperatures at which simulations have been performed (blue circles).

Finally, we compute the temperature at which the relaxation times show an apparent divergence by fitting the data at each density above ϕ_0 , for each dimension, to the Vogel-Fulcher-Tammann (VFT) form, $\tau_\alpha = \tau_0 \exp \left[\frac{1}{K_{VFT} \left(\frac{T}{T_{VFT}} - 1 \right)} \right]$. In Fig. 4, we show the density-temperature diagram for $d = 3$ and $d = 7$ (results for other dimensions are shown in the SM) which shows ϕ_0 and ϕ_J , along with the density dependent T_{VFT} . The results shown illustrate the manner in which the relationship between ϕ_0 and ϕ_J changes with spatial dimension. The T_{VFT} values shown extrapolate to zero at $\phi \rightarrow \phi_0$, illustrating that ϕ_0 is the relevant limit density for the density dependent glass transition.

Conclusion: To summarize, we have studied the dynamics of model glass forming liquids consisting of soft (harmonic) spheres by measuring relaxation times as a function of temperature for several densities for spatial dimensions 3 – 8. The temperature dependence exhibits

a crossover from sub-Arrhenius to super-Arrhenius behavior as density increases. We perform a new scaling analysis of the relaxation times to identify a density ϕ_0 which corresponds to the ideal glass transition density for the hard sphere (or zero temperature) limit. We also estimate the (lowest) jamming density ϕ_J , and show that for $d > 4$, $\phi_0 > \phi_J$. Comparing with theoretical calculations in [15], we find near quantitative agreement with our estimated ϕ_0 values (albeit with a steeper d dependence for the ϕ_0 we obtain), whereas the ϕ_J values we obtain are underestimated in [15]. Our results thus provide a useful benchmark for future efforts in developing quantitative theories of the glass and jamming transitions.

Acknowledgements. We thank Francesco Zamponi, Patrick Charbonneau and Peter Morse for useful discussions, sharing results, and comments on the manuscript. We gratefully acknowledge Anshul Parmar for significant help in setting up the numerical investigations presented in this manuscript. We acknowledge the Thematic Unit of Excellence on Computational Materials Science, and the National Supercomputing Mission facility (Param Yukti) at the Jawaharlal Nehru Center for Advanced Scientific Research for computational resources. SK acknowledges support from Swarna Jayanti Fellowship grants DST/SJF/PSA-01/2018-19 and SB/SFJ/2019-20/05. SS acknowledges support through the JC Bose Fellowship (JBR/2020/000015) SERB, DST (India).

* Corresponding author: sastry@jncasr.ac.in

- [1] P. G. Debenedetti and F. H. Stillinger, *Nature* **410**, 259 (2001).
- [2] K. Binder and W. Kob, *Glassy materials and disordered solids: An introduction to their statistical mechanics* (World scientific, 2011).
- [3] L. Berthier and G. Biroli, *Reviews of Modern Physics* **83**, 587 (2011).
- [4] S. Karmakar, C. Dasgupta, and S. Sastry, *Annu. Rev. Condens. Matter Phys.* **5**, 255 (2014).
- [5] C. P. Royall, F. Turci, S. Tatsumi, J. Russo, and J. Robinson, *Journal of Physics: Condensed Matter* **30**, 363001 (2018).
- [6] A. J. Liu and S. R. Nagel, *Annu. Rev. Condens. Matter Phys.* **1**, 347 (2010).
- [7] S. Torquato and F. H. Stillinger, *Rev. Mod. Phys.* **82**, 3197 (2010).
- [8] R. P. Behringer and B. Chakraborty, *Reports on Progress in Physics* **82**, 012601 (2018).
- [9] P. Charbonneau, J. Kurchan, G. Parisi, P. Urbani, and F. Zamponi, *Annual Review of Condensed Matter Physics* **8**, 265 (2017).
- [10] A. Ikeda, L. Berthier, and P. Sollich, *Physical review letters* **109**, 018301 (2012).
- [11] T. R. Kirkpatrick and D. Thirumalai, *Physical review letters* **58**, 2091 (1987).
- [12] T. Kirkpatrick and D. Thirumalai, *Physical Review A* **37**, 4439 (1988).
- [13] T. R. Kirkpatrick, D. Thirumalai, and P. G. Wolynes, *Physical Review A* **40**, 1045 (1989).
- [14] G. Parisi, P. Urbani, and F. Zamponi, *Theory of Simple Glasses: Exact Solutions in Infinite Dimensions* (Cambridge University Press, 2020).
- [15] M. Mangeat and F. Zamponi, *Physical Review E* **93**, 012609 (2016).
- [16] P. Charbonneau, A. Ikeda, G. Parisi, and F. Zamponi, *Physical review letters* **107**, 185702 (2011).
- [17] P. Charbonneau, A. Ikeda, G. Parisi, and F. Zamponi, *Proceedings of the National Academy of Sciences* **109**, 13939 (2012).
- [18] B. Charbonneau, P. Charbonneau, Y. Jin, G. Parisi, and F. Zamponi, *The Journal of chemical physics* **139**, 164502 (2013).
- [19] L. Berthier, P. Charbonneau, and J. Kundu, *Phys. Rev. Lett.* **125**, 108001 (2020).
- [20] P. Charbonneau and P. K. Morse, *Physical review letters* **126**, 088001 (2021).
- [21] P. Charbonneau and P. K. Morse, *arXiv preprint arXiv:2201.07629* (2022).
- [22] J. D. Eaves and D. R. Reichman, *Proceedings of the National Academy of Sciences* **106**, 15171 (2009).
- [23] S. Sengupta, S. Karmakar, C. Dasgupta, and S. Sastry, *Physical review letters* **109**, 095705 (2012).
- [24] S. Sengupta, S. Karmakar, C. Dasgupta, and S. Sastry, *The Journal of chemical physics* **138**, 12A548 (2013).
- [25] W.-S. Xu, J. F. Douglas, and K. F. Freed, *Adv. Chem. Phys* **161**, 443 (2016).
- [26] M. Adhikari, S. Karmakar, and S. Sastry, *The Journal of Physical Chemistry B* **125**, 10232 (2021), pMID: 34494429, <https://doi.org/10.1021/acs.jpcc.1c03887>.
- [27] C. S. O'Hern, L. E. Silbert, A. J. Liu, and S. R. Nagel, *Phys. Rev. E* **68**, 011306 (2003).
- [28] P. Chaudhuri, L. Berthier, and S. Sastry, *Physical review letters* **104**, 165701 (2010).
- [29] R. J. Speedy, *Journal of Physics: Condensed Matter* **10**, 4185 (1998).
- [30] R. J. Speedy and P. G. Debenedetti, *Molecular Physics* **88**, 1293 (1996).
- [31] F. Krzakala and J. Kurchan, *Physical Review E* **76**, 021122 (2007).
- [32] R. Mari, F. Krzakala, and J. Kurchan, *Physical review letters* **103**, 025701 (2009).
- [33] M. Hermes and M. Dijkstra, *EPL* **89**, 38005 (2010).
- [34] M. Ciamarra, A. Coniglio, and A. D. Candia, *Soft Matter* **6**, 2975 (2010).
- [35] M. Ozawa, T. Kuroiwa, A. Ikeda, and K. Miyazaki, *Physical review letters* **109**, 205701 (2012).
- [36] L. Berthier and T. A. Witten, *EPL (Europhysics Letters)* **86**, 10001 (2009).
- [37] L. Berthier and T. A. Witten, *Physical Review E* **80**, 021502 (2009).
- [38] A. Coniglio, M. P. Ciamarra, and T. Aste, *Soft matter* **13**, 8766 (2017).
- [39] L. Berthier, D. Coslovich, A. Ninarello, and M. Ozawa, *Physical review letters* **116**, 238002 (2016).
- [40] M. P. Ciamarra, M. Nicodemi, and A. Coniglio, *Soft Matter* **6**, 2871 (2010).
- [41] J. Kurchan, G. Parisi, P. Urbani, and F. Zamponi, *The Journal of Physical Chemistry B* **117**, 12979 (2013).
- [42] M. H. Cohen and D. Turnbull, *The Journal of Chemical Physics* **31**, 1164 (1959).
- [43] D. J. Durian, *Physical review letters* **75**, 4780 (1995).
- [44] D. Brown and J. Clarke, *Molecular Physics* **51**, 1243

- (1984).
- [45] See Supplemental Material at [<URL>](#) which contains a description of the procedure used to define the overlap function, the scaling analysis using the scaling function defined by Berthier and Witten, the new effective diameter definition we employ in this work and the corresponding scaling function, comparison of results from the Berthier-Witten scaling function and the one proposed in this work, error analysis for different data collapse procedures employed, details of the procedure used for obtaining jamming densities, comparison of jamming densities obtain with previous work, the density-temperature phase diagram for all the dimensions investigated, and the statistics of rattlers, which contains the additional reference [?].
- [46] R. W. Hall and P. G. Wolynes, *The Journal of chemical physics* **86**, 2943 (1987).
- [47] G. Brambilla, D. El Masri, M. Pierno, L. Berthier, L. Cipelletti, G. Petekidis, and A. B. Schofield, *Physical review letters* **102**, 085703 (2009).
- [48] V. Baranau and U. Tallarek, *AIP Advances* **10**, 035212 (2020).
- [49] M. Maiti and M. Schmiedeberg, *Journal of Physics: Condensed Matter* **31**, 165101 (2019).
- [50] J. A. Barker and D. Henderson, *The Journal of chemical physics* **47**, 4714 (1967).
- [51] P. K. Morse and E. I. Corwin, *Phys. Rev. Lett.* **112**, 115701 (2014).
- [52] A. Manacorda and F. Zamponi, *arXiv preprint arXiv:2201.01161* (2022).